UiO : Department of Physics
University of Oslo

Approximating the ${}^1S_0$ Partial Wave of Nucleon-Nucleon Scattering With Effective Field Theory

Erlend Lima

December 18, 2020

Abstract

GitHub repository: https://github.com/ErlendLima/NuclearForces

Contents

1 Introduction

2 Theory

2.1 Effective Field Theory

The quantum field theory developed in the 1930s and 1940s had The formalism of computing Feynman diagrams led to difficulties when working with loops. Infinities pop up left, right and center, giving nonsensical results. A formalism was developed by Feynman, Schwinger, Tomonaga and Dysin [ref] to nevertheless obtain sensible values through systematically canceling infinities. Despite the impressive agreement with experiments [ref], many [who?] felt icky about the method, afraid it was nothing more but a mathematical trick, and our failure to understand it implied a failure to understand the physical significance.

It wasn't before 1970s[when?] that Ken Wilson, an otherwise unknown physicist, illuminated the issue [ref]. The loop diagrams gave infinities because one has to sum over all possible [diagrams. clumsy structure, rewrite], for all energies. However, we do not know that QFT is the correct theory for high energy physics, nor is it necessary to assume so in order to do calculations at lower energies. One can instead set an arbitrary[not practically arbitrary, make clearer] limit Λ above which is the high energy, or *ultraviolet* (UV), regime, and below which is the low energy, or *infrared* (IR), regime [det ble nøstes. nøst opp]. Ken Wilson argued it is better we admit the physics of UV is unknown and treat it as such, and instead develop a low energy model. That the physics of UV is irrelevant can be seen from the fact that any low energy model has many consistent high energy models, or *completions* [ref]. This gave rise to *effective field theories* (EFT).

A more or less general procedure was developed to generate an EFT[1, p. 7]:

1. Identify the soft and hard scales, and the degrees of freedom appropriate for (low-energy) nuclear physics.
2. Identify the relevant symmetries of low-energy QCD and investigate if and how they are broken.
3. Construct the most general Lagrangian consistent with those symmetries and symmetry breakings.
4. Design an organizational scheme that can distinguish between more and less important contributions: a low-momentum expansion.
5. Guided by the expansion, calculate Feynman diagrams for the problem under consideration to the desired accuracy.

[seems out of place, as all steps except 5. are intractable by me]

2.2 The Chiral Lagrangian

In QCD the Lagrangian is[1, p. 7]

$$\mathcal{L}_{\text{QCD}} = \bar{q}(i\gamma^\mu \mathcal{D}_\mu - \mathcal{M})q - \frac{1}{4}\mathcal{G}_{\mu\nu,a}\mathcal{G}_a^{\mu\nu}$$

with $\mathcal{D}_\mu = \partial_\mu - ig\frac{\lambda_a}{2}\mathcal{A}_\mu, a$ the gauge-covariant derivative, $\mathcal{G}_{\mu\nu,a}$ the gluon field strength tensor, q the quark fields and $\mathcal{M}$ the quark mass matrix.

[vanishing quark mass]

[short about chiral symmetry]

[explicit and spontaneous symmetry breaking]

[chiral effective Lagrangian]

In QCD the u and d quarks have approximately chiral symmetry. Explicelty broken because u and d do not have the same mass Spontaneously broken

Rekkeutvikling av Lpipi

Chiral order

2.3 One Pion Exchange Force

We obtain

$$V(\vec{r}) = \frac{f_\pi^2}{m_\pi^2}\left[C_\sigma \sigma \cdot \sigma_2\right]$$

$$V^{LO}(\vec{q},\vec{k}) = C_s + C_t \vec{\sigma_a} \cdot \vec{\sigma_2}$$

$$V^{NLO}(\vec{q},\vec{k}) = C_1\vec{q}^2 + C_2\vec{k}^2 + \vec{\sigma}_1 \cdot \vec{\sigma}_2 + iC_5\frac{\vec{\sigma}_1 + \vec{\sigma}_2}{2} \cdot \vec{q} \times \vec{k} + C_6\vec{q} \cdot \vec{\sigma}_1\vec{q} \cdot \vec{\sigma}_2 + C_7\vec{k} \cdot \vec{\sigma}_1\vec{k} \cdot \vec{\sigma}_2$$

where $\vec{q} = \vec{p} - \vec{p}'$ is the momentum transfer, $= \frac{\vec{p}+\vec{p}'}{2}$ the average momentum, and $\vec{p}$ and $\vec{p}'$ the relative momenta.

[Regularization]

$$V(p', p) \xrightarrow[\text{regularize}]{} f_\Lambda(p')V(p', p)f_\Lambda(p)$$

where [why? Fourier transform trick]

$$f_\Lambda(p) = \exp\{-p^4/Lambda^4\}$$

Listing 1 Implementation of the EFT potentials.

```
#= EFT Potentials =#
#= Lowest leading order pionless EFT potential =#
struct LO <: Potential
    C₀::Float64
end

function (V::LO)(k, k′)
    V.C₀
end

#= Next leading order pionless EFT potential =#
struct NLO <: Potential
    C₀::Float64
    C₂::Float64
end

function (V::NLO)(k, k′)
    V.C₀ + V.C₂*(k^2 + k′^2)
end

#= Next next leading order pionless EFT potential =#
struct NNLO <: Potential
    C₀::Float64
    C₂::Float64
    C₄::Float64
end

function (V::NNLO)(k, k′)
    V.C₀ + V.C₂*(k^2 + k′^2) + V.C₄*(k^4 + k′^4) + V.C₄*k^2*k′^2
end


#= Pion interaction =#
struct Pion <: Potential
    mπ::Float64
    Vπ::Float64
end
Pion(Vπ::Real) = Pion(0.7, Vπ)

function (V::Pion)(k, k′)
    mπ = V.mπ
    V.Vπ/(4mπ * k*k′) * log((mπ^2 + (k+k′)^2)/(mπ^2 + (k-k′)^2))
end
```

Listing 2 CompoundPotential used to add a pionic term to a pionless potential, among other uses.

```
struct CompoundPotential <: Potential
    V1::Potential
    V2::Potential
end

function(V::CompoundPotential)(r)
    V.V1(r) + V.V2(r)
end

function(V::CompoundPotential)(k, k′)
    V.V1(k, k′) + V.V2(k, k′)
end

+(V1::Potential, V2::Potential)::Potential = CompoundPotential(V1, V2)
```

3 Method

3.1 Code Implementation

Extending the previous Scattering.jl library to handle the potentials spawned by effective field theory is a simple matter. Each potential corresponds to a struct with the necessary coefficients, along with a callable method for evaluating the potential. These are shown in Listing 1.

Adding one-pion exchange term to the pionless potentials is done by a combining a pionless potential with the one-pion exchange potential through a CompoundPotential, its implementation shown in Listing 2

Finally, a potential can be regularized with the smooth UV regulator [ref] by sandwiching a potential with the f_Λ factors, as implemented in Listing 3.

Listing 3 Regularization is too a Potential wrapped around another Potential.

```
#= UV Regulatization =#
struct UVRegulator <: Potential
    V::Potential
    Λ::Float64  # Cutoff parameter [fm⁻¹]
end

function (V::UVRegulator)(k, k′)
    exp(-k^4/V.Λ^4) * V.V(k, k′) * exp(-k′^4/V.Λ^4)
end
```

3.2 Minimization Procedure

[fix. Modern works are much more detailed]Earlier works on the same topic [ref lepage,machleidt,more] often skimp on detailing the methods used to obtain the coefficients for the potentials. As a counterweight, the following is a detailed explanation of the minimization employed here.

[This section may be rewritten once I've understood EKM]

Potentials derived from effective field theory are most accurate at low energies, i.e. the low infrared region. By construction, a fit here should give the best overall fit for all energies in the infrared region. However, the phase shift of the Reid potential is near linear for $E < 5$ MeV, before the peak. The more degrees of freedom a parameterized potential has, the more trouble minimization procedures will have in finding good coefficients that generalize without being able to see more features. It is therefore to expect that potentials with more degrees of freedom require data from higher and higher energies to perform a good fit.

Fitting to higher energies is undesirable as the EFT potentials quickly break down. To find an optimal fit it is therefore necessary to let the final energy E_{end} used in the fit be a free parameter which itself is optimized. In addition, a bias is introduced to weight the low energy points more by using logarithmically spaced points.

Any form of fitting procedure require a measure of the error. A common measure is the square of the residuals, $(y_i - \text{fit}_i)^2$, used in least squares and χ^2 minimization. This is not necessarily optimal for our problem because the potentials derived from EFT are asymptotically good as $k \to 0$, and so one would expect the fit to get progressively worse as the energy increases. Using the square of the residuals the error at high energies will then weight considerably more than the error at low energies, biasing the fit for a better "global" fit. A better choice might be to use the absolute error of the residuals $|y_i - \text{fit}_i|$, or the relative error $\frac{|y_i - \text{fit}_i|}{y_i}$. Doing so runs the cost of slower minimization as many solvers rely on the properties of the square of residuals to perform their minimization.

This sends us to the problem of which minimization procedure to use. As we are using the Reid potential as the Truth, we need not care for empirical errors, only about obtaining a good fit in a reasonable amount of time. This turns out to be substantially more difficult that what it seems at face value. There are two reasons for this. The first is that the parameter space increases rapidly from 1 for LO to 4 with NNLO. Letting Λ vary adds another parameter, and so does adding a pionic interaction. Not only does this make the solution space more shallow[ref bayes], it also introduces several local minima. Having obtained one solution, one can not set aside the fear that the solution is suboptimal, and many methods make it difficult to measure how much of the parameter space one has explored. Trials showed that gradient-based methods easily get stuck and many methods using exorbitant amount of time to obtain convergence. Simulated annealing[ref] found very good fits, but only after running for hours.

Another problem arises from the K-matrix method used to compute the phase shift. There is an inherent limitation to the method as the computation of δ perform an atan, setting an upper bound of $\pi/2$. Unfortunate values of the parameters or their combination lead

[Holding Λ constant]

[Region of fit]

4 Results and Discussion

4.1 Fit at Low Energies

As recommended by [machleidth], a fit is performed in the range $[10^{-3}, 10^{-1}]$ MeV. The resulting phase shift and relative error in the range 10^{-3} to 100 MeV is shown in Fig. 4.1. Each order has less error than the previous in the fit region, converging to the same error as the energy increases. There is, however, not a massive improvement from NLO to NNLO, especially when comparing to figure 3 of [machleidt, show here for reference]. Note also the different shapes of the error curves. Each dip corresponds to a change in sign of the error, a crossing of the computed phase shift with the actual phase shift.

The two phase shift results of NNLO illustrate a common problem with our method of fitting. A completely unconstrained fit, labeled simply "NLO", give worse results than a constrained fit, labeled "NLO Constrained", where the coefficients are forced to be within some hand picked regions. The reason for this is not clear, but is discussed later.

The 95% confidence intervals (CI) of each coefficient is given in

	Coefficients			
Potential	C_0	C_2	C_4	C_4'
LO	-0.53	—	—	—
NLO	-0.54	0.048	—	—
NNLO	-0.50	0.054	-0.99	0.87
NNLO Constrained	-0.52	0.37	-1.18	-1.85

	95% Confidence Interval			
	C_0	C_2	C_4	C_4'
LO	2×10^{-6}	—	—	—
NLO	1×10^{-5}	6×10^{-5}	—	—
NNLO	3×10^{1}	7×10^{1}	6×10^{2}	1×10^{3}
NNLO Constrained	2×10^{1}	4×10^{1}	4×10^{2}	7×10^{2}

Table 4.1: *Coefficients found from fit at 10^{-3} to 10^{-1} MeV, as well as 95% confidence intervals of the coefficients. Only the rough magnitude is shown for the CI as the numbers change with each execution of the fit. [Labels refuse to align. Fix].*

4.2 Fit at Medium Energies

To see the effect of including higher energies, another fit was performed from 10^{-3} to 1 MeV. The resulting phase shifts and errors are shown in Fig. 4.2. There is a degradation all around except around 1 MeV when compared to the low energy fit. In particular, NLO is far worse, being negligibly better than LO. Another noteworthy change is the increasing number of dips in the NNLO error, suggesting a more complex shape of the phase shift, as well as NNLO being better able to fit the Reid potential at energies higher than 1 MeV.

The coefficients and CI are shown in Table 4.2. The degradation in LO and NLO is reflected in the increased uncertainty of the coefficients by some orders of magnitude. The CIs of NLO are still small when compared to the value of the coefficient, indicating that the region

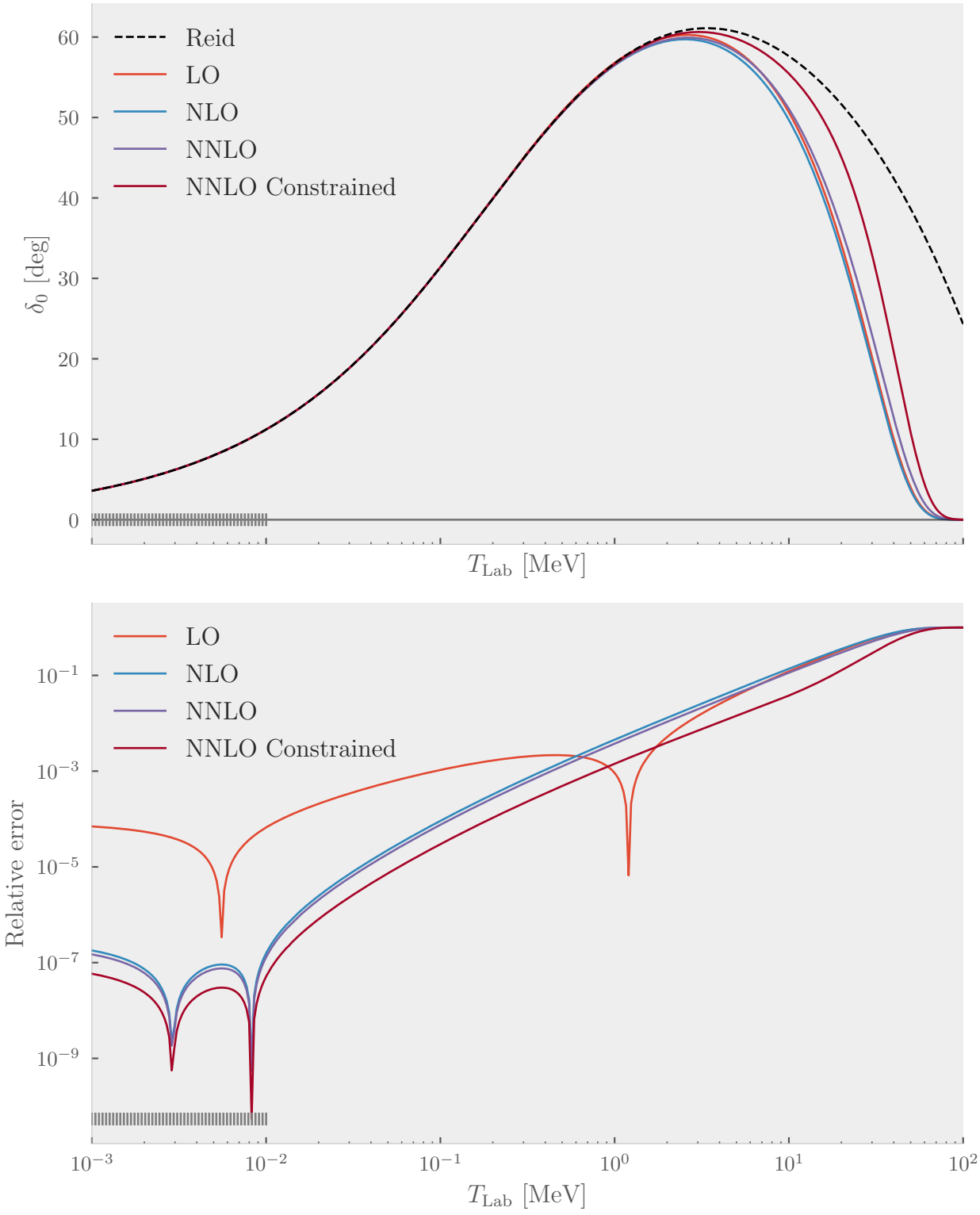

Figure 4.1: *Fit to low energy region with the phase shift shown in the top panel and relative error in the lower. The points used in the fit is indicated as ticks near the bottom of each plot. LO, NLO and NNLO had no limits to their coefficients, while NNLO Constrained was constrained to exclude "unphysical" phase shifts. The sharp dips are where the curves change sign.*

used in the fit is worse than the lower energy. On the other hand, the NNLO has markedly smaller CIs, indicating that the higher energies are necessary for a good fit.

	Coefficients			
Potential	C_0	C_2	C_4	C_4'
LO	-0.53	—	—	—
NLO	-0.53	0.015	—	—
NNLO	-0.46	0.44	-2.4	-1.1

	95% Confidence Interval			
	C_0	C_2	C_4	C_4'
LO	1×10^{-5}	—	—	—
NLO	1×10^{-3}	6×10^{-3}	—	—
NNLO	4×10^{-1}	6×10^{-1}	5	1×10^{1}

Table 4.2: *Coefficients found from fit at 10^{-3} to 1 MeV, as well as 95% confidence intervals of the coefficients. Only the rough magnitude is shown for the CI as the numbers change with each execution of the fit. [Labels refuse to align. Fix].*

4.3 High at High Energies

Yet another fit was performed at energies 10^{-3} to 100 MeV, with results shown in Fig. 4.3, and yet again we see increase in the relative error. All of the phase shift curves markedly deviate from the phase shift of the Reid potential. Of the three, NLO has the worst performance, while the simplest, LO, performs the best.

Table 4.3 gives the CIs of the coefficients. The same tale repeats, with CI becoming increasingly wide. The CIs of the coefficients of NNLO are utterly useless, spanning six and eight orders of magnitude. It shows that the least squares method fails at finding any fitting coefficients. Precisely why it fails is discussed later in 4.5.

	Coefficients			
Potential	C_0	C_2	C_4	C_4'
LO	-0.53	—	—	—
NLO	-0.40	-0.58	—	—
NNLO	-0.70	1.3	-3.0	-9.6

	95% Confidence Interval ($\pm$)			
	C_0	C_2	C_4	C_4'
LO	3×10^{-2}	—	—	—
NLO	1×10^{-1}	6×10^{-1}	—	—
NNLO	2×10^{6}	3×10^{6}	1×10^{8}	1×10^{8}

Table 4.3: *Coefficients found from fit at 10^{-3} to 100 MeV, as well as 95% confidence intervals of the coefficients. Only the rough magnitude is shown for the CI as the numbers change with each execution of the fit. [Labels refuse to align. Fix].*

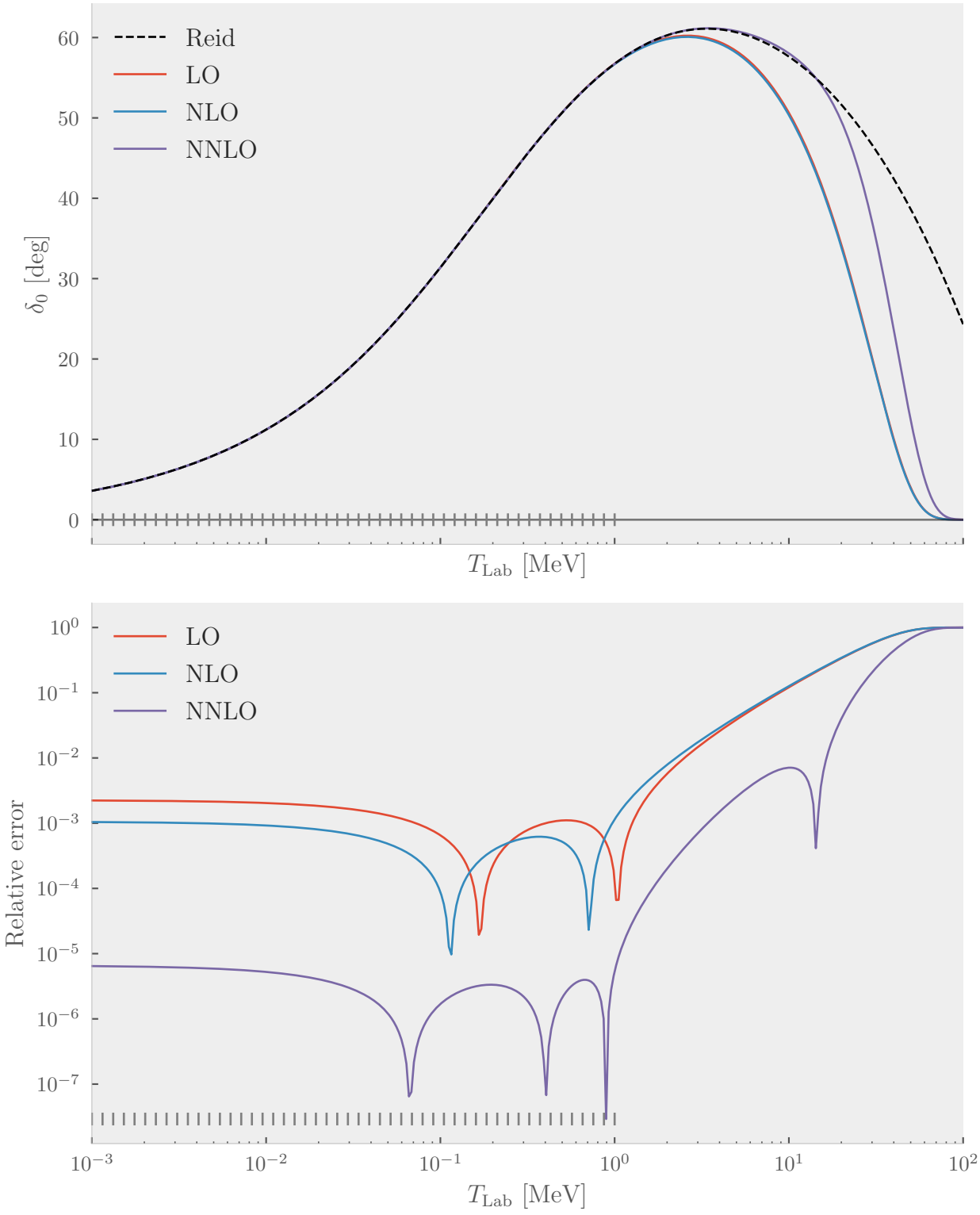

Figure 4.2: *Fit to the mid energy region with the phase shift shown in the top panel and relative error in the lower. The points used in the fit are indicated as ticks near the bottom of each plot. No constraints were used on the coefficients. When compared to the low energy fit, all perform worse in low energy region. NLO does negligibly better than LO.*

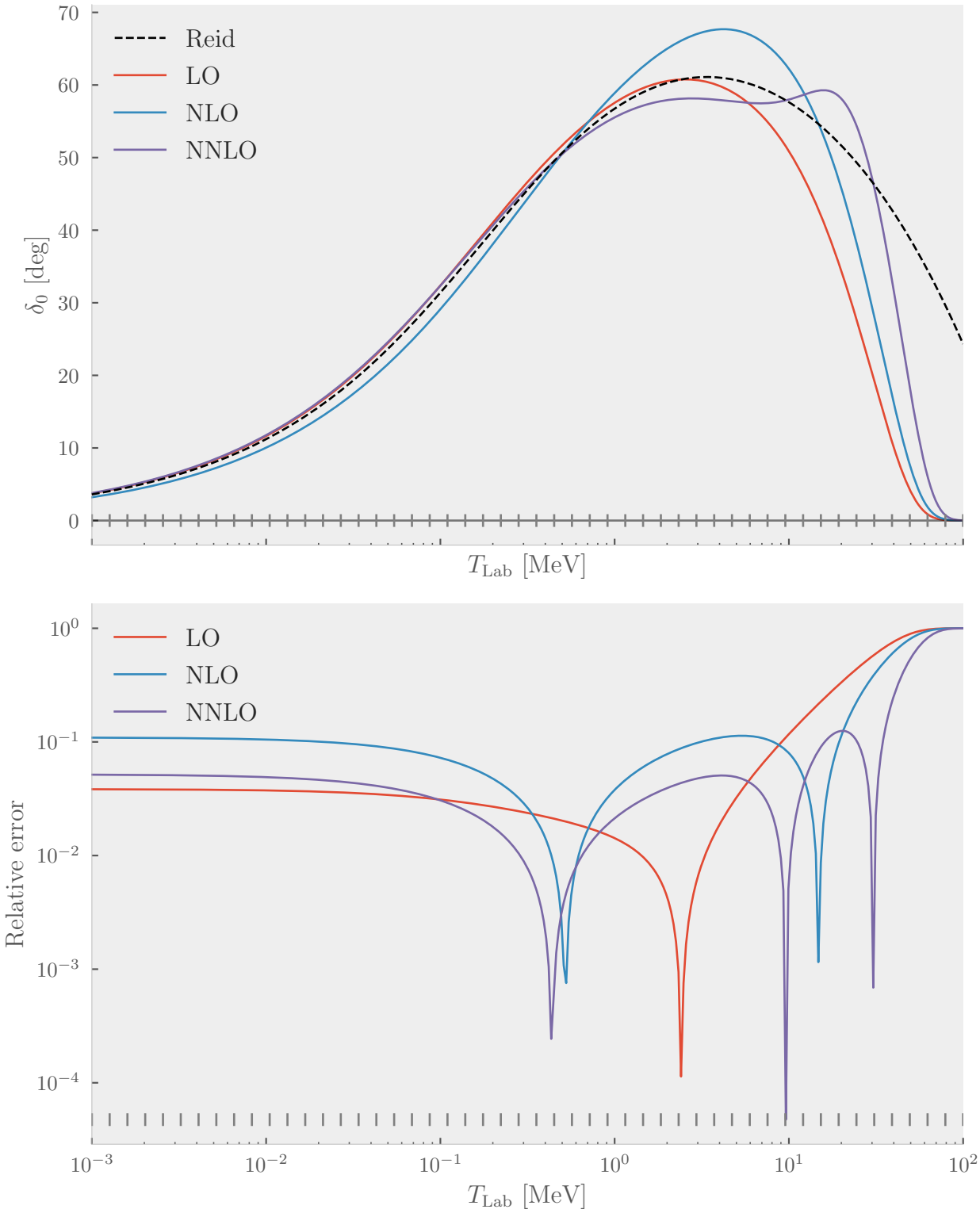

Figure 4.3: *Fit to the high energy region with the phase shift shown in the top panel and relative error in the lower. The points used in the fit are indicated as ticks near the bottom of each plot. The errors are several order of magnitude greater when compared to Fig. 4.1 and Fig. 4.2*

4.4 Dependence on Fit Region

Since there seems to be no consensus for what the best fit region is, several regions were used when fitting the coefficients. LO is consistently well behaved, with fast convergence for the minimization procedures and small dependence on the hyperparameters.

4.5 Breakdown of the K-Matrix method

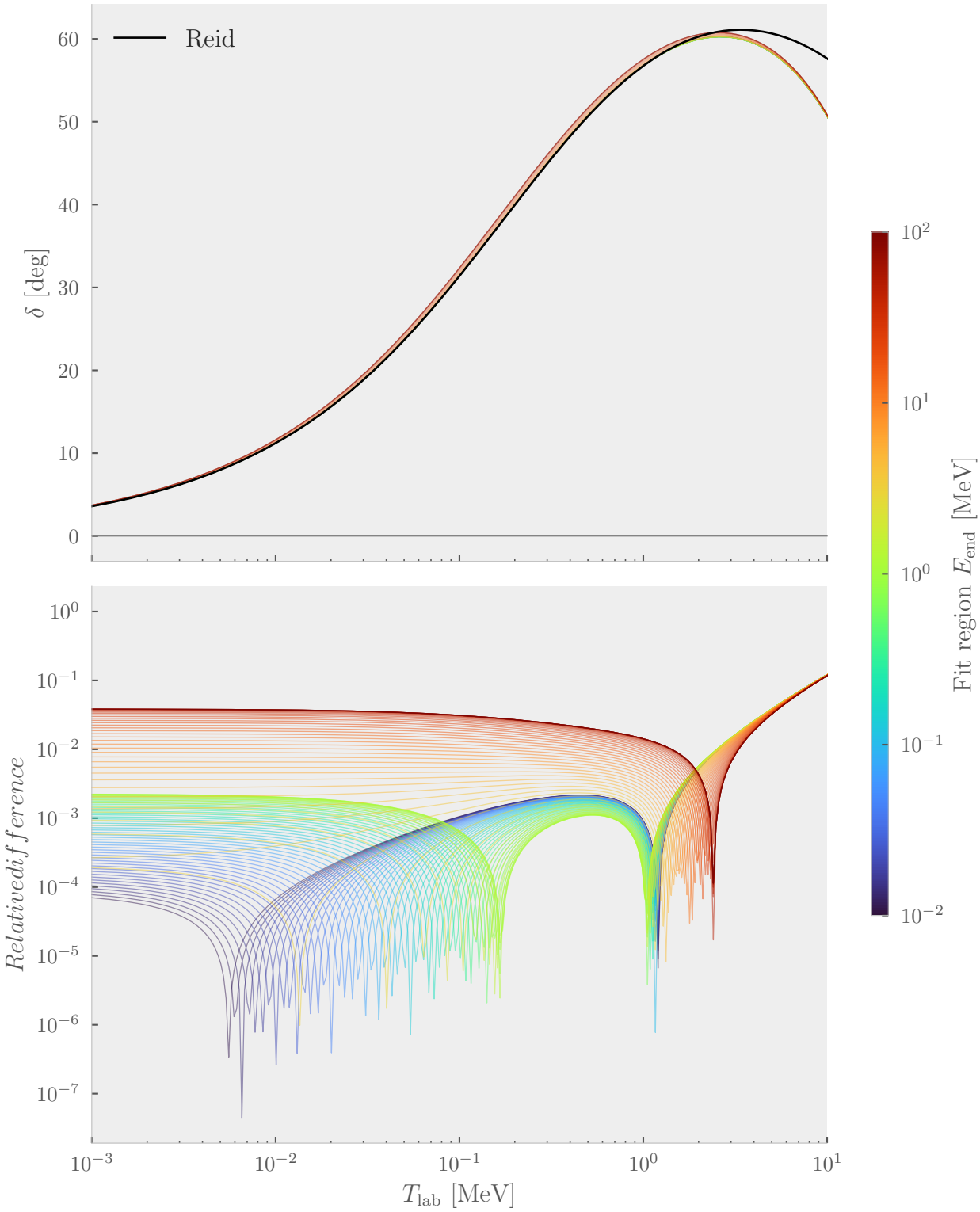
Reid
60
50
40
30
20
10
0
δ [deg]
10^0
10^{-1}
10^{-2}
10^{-3}
10^{-4}
10^{-5}
10^{-6}
10^{-7}
$Relativedifference$
10^{-3}
10^{-2}
10^{-1}
10^0
10^1
T_{lab} [MeV]
10^2
10^1
10^0
10^{-1}
10^{-2}
Fit region E_{end} [MeV]

Figure 4.4

5 Conclusion

References

[1] R. Machleidt and D.R. Entem. "Chiral effective field theory and nuclear forces". In: *Physics Reports* 503.1 (June 2011), pp. 1–75. ISSN: 0370-1573. DOI: 10.1016/j.physrep.2011.02.001. URL: http://dx.doi.org/10.1016/j.physrep.2011.02.001 (cit. on p. 2).